Journal of Alloys and Compounds 509S (2011) S779–S781

Contents lists available at ScienceDirect

Journal of Alloys and Compounds

journal homepage: www.elsevier.com/locate/jallcom

Hydrogenation of TiNi shape memory alloy produced by mechanical alloying

Takeshi Saito[a,*], Tomonori Yokoyama[a], Akito Takasaki[b]

[a] *Graduate School of Engineering, Shibaura Institute of Technology, 3-7-5 Toyosu, Koto-ku, 135-8548 Tokyo, Japan*
[b] *Department of Engineering Science and Mechanics, Shibaura Institute of Technology, 3-7-5 Toyosu, Koto-ku, 135-8548 Tokyo, Japan*

ARTICLE INFO

Article history:
Received 17 July 2010
Received in revised form 19 October 2010
Accepted 22 October 2010
Available online 4 November 2010

Keywords:
TiNi shape memory alloy
Hydrogen
Martensitic transformation
X-ray diffraction
Mechanical alloying

ABSTRACT

TiNi intermetallic compounds, produced by a combination of mechanical alloying and direct current sintering, were hydrogenated at several hydrogen pressures at 473 K for 4 h to investigate their hydrogen desorption and martensitic transformation behaviors. The microstructures and the hydrogen desorption properties were dependent on levels of hydrogen concentrations. The crystal lattice of TiNi (B2) phase expanded and TiNi hydride formed with an increase in hydrogen pressure. Two stage martensitic and reverse transformations were observed at low hydrogen concentration. An enthalpy of martensitic transformation was lower than that of reverse transformation. TiNi (martensite) phase was confirmed at intermediate hydrogen concentration, suggesting that hydrogen-induced martensitic transformation occurred during hydrogenation. No martensitic and reverse transformations occurred at high hydrogen concentration because of the hydride formation.

1. Introduction

TiNi alloys have shape memory effect due to thermoelastic martensitic transformation between TiNi (B2) parent and monoclinic martensitic phases. The martensitic transformation behaviors are likely to be sensitive to substitutional elements, solute elements and impurities in the TiNi (B2) matrix. Effect of hydrogen on the martensitic transformation has been studied by several researchers. However, the conclusions are still controversial. A multiple stage transformation was reported after hydrogenation although a single transformation was observed before hydrogenation [1]. While the martensitic transformation temperature was reported to be lowered by cathodic hydrogen charging [2], there were some reports that the transformation temperature was insensitive to hydrogenation [3,4]. Although disproportional reaction (formation of TiH_2 phase, $TiNi_3$ phase and Ni) was observed after hydrogenation [5], Burch and Mason [6] and Yokoyama et al. [7] attained TiNi hydride phase. Pelton et al. [8] reported that R-phase or TiNi (martensite) phase was induced during hydrogenation. Such controversial conclusions were thought to arise from different levels of hydrogen concentrations. Thus, it is important to investigate a process of hydrogenation and the martensitic transformation behaviors for the TiNi (B2) phase at different levels of hydrogen concentrations. We have already reported a production of TiNi powder alloy by mechanical alloying (MA) [9] and the bulk alloy by a subsequent direct current sintering [10]. In this study, influence of hydrogen on the martensitic transformation behaviors of the TiNi bulk alloy produced by a combination of MA and direct current sintering was investigated.

2. Experimental procedure

A bulk sample with the chemical composition of $Ti_{50}Ni_{50}$ (at.%) was synthesized by a combination of MA and direct current sintering. The details of experimental conditions have previously been reported [9,10]. Gaseous hydrogenation was conducted at several hydrogen pressures (0.5, 1.0, 2.0 and 3.0 MPa) at 473 K for 4 h to control hydrogen concentrations in the samples by using a high-pressure stainless vessel. The crystal structures of the samples were determined by X-ray diffraction (XRD) equipment (Rigaku Ultima IV) using Cu-Kα radiation at 40 kV and 45 mA with a graphite monochromator at room temperature. The Rietveld refinement of the XRD patterns was carried out with the *Fullprof* program [11]. The hydrogen desorption temperature was measured by thermal desorption spectroscopy (TDS) (ULVAC TDS-M202P) under high vacuum condition (10^{-6} Pa) at a heating rate of 10 K/min. The martensitic transformation temperature was measured by differential scanning calorimetry (DSC) (Shimadzu DSC-60) under argon gas flow (300 ml/min) at heating and cooling rates of ±5 K/min.

3. Results and discussion

TiNi (B2) ($a = 0.301$ nm) phase with a small amount of Ti_2Ni ($a = 1.108$ nm) and $TiNi_3$ ($a = 0.511$ nm and $c = 0.834$ nm) phases was obtained in the as-synthesized bulk sample. Martensitic and reverse transformations were observed for the bulk sample. The transformation temperatures were 282 K, 264 K, 279 K and 295 K for M_s, M_f, A_s and A_f, respectively, where M_s is start temperature for the martensitic transformation, M_f is finish temperature for the martensitic transformation, A_s is start temperature for the reverse

---

[*] Corresponding author at: Materials Science and Engineering Lab, Department of Engineering Science and Mechanics, Shibaura Institute of Technology, 3-7-5 Toyosu, Koto-ku, 135-8548 Tokyo, Japan. Tel.: +81 3 5859 8059; fax: +81 3 5859 8001.

E-mail address: m408030@shibaura-it.ac.jp (T. Saito).

0925-8388/$ – see front matter © 2010 Elsevier B.V. All rights reserved.
doi:10.1016/j.jallcom.2010.10.128

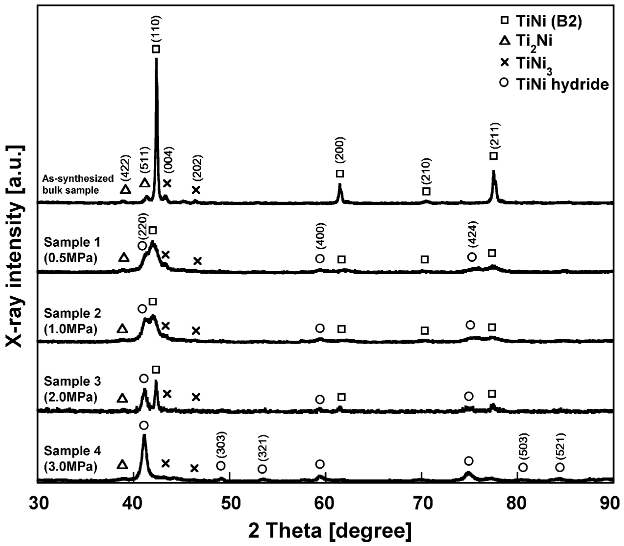

Fig. 1. XRD patterns for the as-synthesized bulk sample and the sample hydrogenated at several hydrogen pressures.

transformation and A_f is finish temperature for the reverse transformation. The transformation enthalpy was calculated to be 1.65 J/g. The bulk sample was hydrogenated in this study.

Fig. 1 shows XRD patterns for the as-synthesized bulk sample and the samples after hydrogenation at hydrogen pressures of 0.5, 1.0, 2.0 and 3.0 MPa. Hereafter, the samples after hydrogenation at hydrogen pressures of 0.5, 1.0, 2.0 and 3.0 MPa are represented as Samples 1, 2, 3 and 4, respectively. The XRD intensities of the TiNi (B2) phase decreased with increasing hydrogen pressure. The XRD peaks at around $2\theta = 42°$ for Samples 1 and 2 were broad, because the XRD peaks for the TiNi (B2) and TiNi hydride ($a = 0.622$ nm and $c = 1.228$ nm) phases were overlapped. Namely, lattice expansion of the TiNi (B2) phase due to diffusion of hydrogen atoms and formation of the TiNi hydride phase occurred simultaneously in the sample. The formation of the TiNi hydride phase became clearer for Sample 3. The TiNi hydride phase formed completely for Sample 4. Bratanich et al. [5] reported a formation of TiH_2 phase, $TiNi_3$ phase and Ni after hydrogenation, which is probably because of an oxide in the sample before hydrogenation.

Hydrogen desorption spectra, measured by TDS, for Samples 1, 3 and 4 are shown in Fig. 2. Two prominent peak temperatures were observed at around 500 and 770 K. It is implied that there are

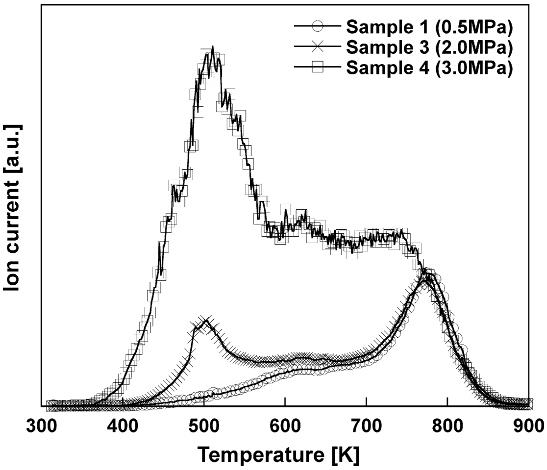

Fig. 2. Hydrogen desorption spectra measured by TDS for the sample hydrogenated at hydrogen pressures of 0.5, 2.0 and 3.0 MPa (Samples 1, 3 and 4).

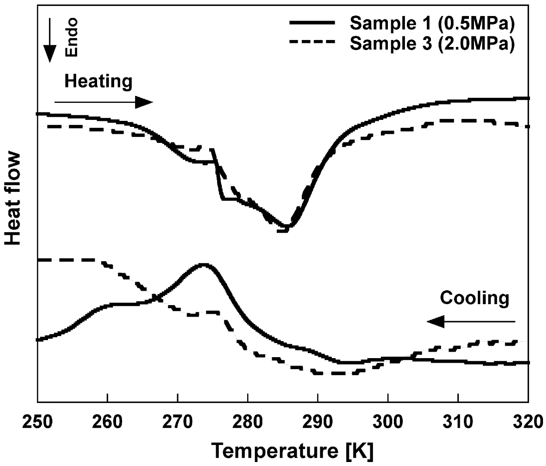

Fig. 3. DSC curves for the sample hydrogenated at hydrogen pressures of 0.5 and 2.0 MPa (Samples 1 and 3).

two kinds of hydrogen sites corresponding to two binding energies. A peak at around 770 K was dominant for Sample 1. The desorption spectrum for Sample 2 was very similar to that for Sample 1. The other peak at around 500 K appeared additionally for Samples 3 and 4. According to a structural analysis for TiNi hydride [12], hydrogen atoms occupy an octahedral position coordinated with two Ni and four Ti atoms. Yokoyama et al. [7] reported that hydrogen in the TiNi hydride desorbed at comparatively low temperatures (room temperature to 473 K). Thus, the prominent peak at around 500 K was attributed to hydrogen in the octahedral position of the TiNi hydride. The other peak at around 770 K was thought to arise from hydrogen evolution from grain boundary or defects, or decomposition of hydrides of the minor phases (Ti_2Ni and $TiNi_3$). The activation energy for hydrogen desorption can be estimated from the shift of desorption peak temperature measured at different heating rates. This measurement is in progress. The results will be reported elsewhere.

DSC curves for Samples 1 and 3 are shown in Fig. 3. Martensitic (exothermic) and reverse (endothermic) transformations were observed. The martensitic and reverse transformation enthalpies for the Sample 1 were the same, which was calculated from an area of the peaks to be 0.69 J/g. The obtained enthalpies are lower than those of the as-synthesized sample (1.65 J/g). It was due to formation of the TiNi hydride phase which does not show any martensitic transformation behavior. Note that two stage martensitic and reverse transformations were observed in Sample 1 although the single martensitic and reverse transformations were observed in the as-synthesized sample. The trapped hydrogen in grain boundary or defects was thought to interrupt the transformation behaviors. The minor phases (Ti_2Ni and $TiNi_3$) could also be assumed to affect the transformation behaviors after hydrogenation. A DSC curve for Sample 2 was very similar to that for Sample 1. The enthalpies of the martensitic and reverse transformations for Sample 3 were calculated to be 0.07 J/g and 0.65 J/g, respectively. The enthalpy of the martensitic transformation was much lower than that of the reverse transformation. This difference in the enthalpies was assumedly attributed to hydrogen-induced martensitic transformation, that is, TiNi (martensite) phase was induced during hydrogenation. (The TiNi (martensite) phase re-transformed to the TiNi (B2) phase after first heating of DSC measurement.) Approximately 13% of the TiNi (martensite) phase was estimated by calculation of the enthalpies difference. Pelton et al. [8] reported that hydrogenation of the TiNi (B2) phase could induce R-phase or martensitic transformations at hydrogen concentration of 6028 mass ppm, suggesting that hydrogen concentration

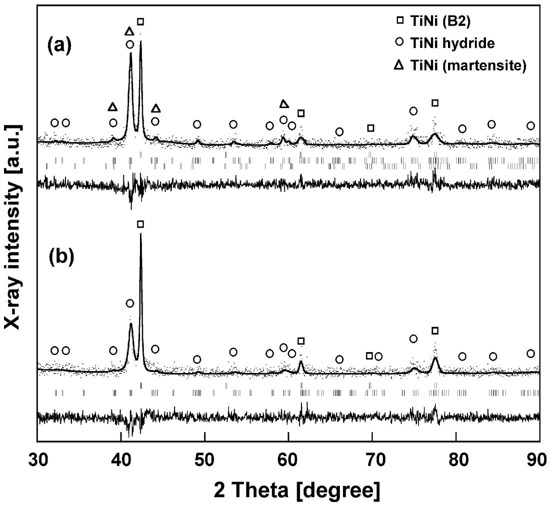

Fig. 4. XRD patterns after Rietveld refinement for Sample 3 (a) after hydrogenation (b) and a DSC cycle of martensitic and reverse transformations.

for Sample 3 might be around 6000 mass ppm. No martensitic and reverse transformations were confirmed in the Sample 4 because of the TiNi hydride formation. The hydrogen concentration for Sample 4 was assumed to be ~13,000 mass ppm because the maximum hydrogen concentration in the TiNi hydride was reported to be 13,000 mass ppm [6]. It is suggested that hydrogenation of the TiNi (B2) phase brings about three kinds of influences on the martensitic and reverse transformations depending on hydrogen concentrations: two stage martensitic and reverse transformations at lower hydrogen concentration (~6000 mass ppm), hydrogen-induced martensitic transformation at intermediate hydrogen concentration (around 6000 mass ppm), and no martensitic transformation at higher hydrogen concentration (~13,000 mass ppm).

Fig. 4(a) shows XRD patterns after Rietveld refinement for the Sample 3. The Rietveld refinements were performed assuming that the TiNi (B2), TiNi hydride and TiNi (martensite) phases, using space groups of *Pm3m*, *I4/mmm* [12,13] and *P2₁/m* [14], respectively. The amount ratios of the TiNi (B2), TiNi hydride and TiNi (martensite) phases were estimated to be 31%, 58% and 11%, respectively. Fig. 4(b) shows XRD patterns after Rietveld refinement after a DSC cycle of martensitic and reverse transformations for the Sample 3. The TiNi (B2) and TiNi hydride phases were confirmed, but no TiNi (martensite) phase. The amount ratios of the TiNi (B2) and TiNi hydride were estimated to be 45% and 55%, respectively. It is implied that the TiNi (martensite) phase (11%) re-transformed to the TiNi (B2) phase completely because of the DSC cycle. This is in good agreement with DSC results.

4. Conclusions

Hydrogen desorption and martensitic transformation behaviors of hydrogenated bulk TiNi intermetallic compounds, produced by a combination of MA and direct current sintering, with different levels of hydrogen concentrations were investigated. The crystal lattice of TiNi (B2) phase gradually expanded and TiNi hydride also formed with an increase in hydrogen pressure. Accelerated hydrogen desorption occurred at around 500 K and 770 K. The two stage martensitic and reverse transformations were observed in the sample hydrogenated at low hydrogen concentration. Although the enthalpies of the martensitic and reverse transformations were the same in the sample hydrogenated at low hydrogen concentration, the enthalpy of the martensitic transformation was lower than that of the reverse transformation in the sample hydrogenated at intermediate hydrogen concentration. TiNi (martensite) phase was induced by hydrogenation at intermediate hydrogen concentration. No martensitic and reverse transformations were confirmed at high hydrogen concentration because of formation of the TiNi hydride completely.

References

[1] T. Ohba, F. Yanagita, M. Mitsuka, T. Hara, K. Kato, Mater. Trans. 43 (5) (2002) 798–801.
[2] W. Jihong, Z. Xiaotao, W. Zhiguo, L. Yanzhang, Rare Met. 24 (2) (2005) 190–193.
[3] C. Damiani, J.L. Pelegrina, M. Ahlers, J. Alloys Compd. 284 (1999) 243–250.
[4] A. Rotini, A. Biscarini, R. Campanella, B. Coluzzi, G. Mazzolai, F.M. Mazzolai, Scripta Mater. 44 (2001) 719–724.
[5] T.I. Bratanich, O.I. Get'man, V.D. Dobrovol'skii, L.I. Kopylova, N.A. Krapivka, T.V. Permyakova, V.V. Skorokhod, Powder Metall. Met. Ceram. 45 (2006) 582–587.
[6] R. Burch, N.B. Mason, J. Chem. Soc., Faraday Trans. 2602 (3) (1979) 561–577.
[7] K. Yokoyama, T. Ogawa, K. Takashima, K. Asaoka, J. Sakai, Mater. Sci. Eng. A 466 (2007) 106–113.
[8] A.R. Pelton, C. Trepanier, X.Y. Gong, A. Wick, K.C. Chen, Proceeding for ASM Materials & Processes for Medical Devices Conference, 2003, http://www.nitinol.com/media/reference-library/006.pdf.
[9] A. Takasaki, Phys. Stat. Sol. (a) 169 (1998) 183–191.
[10] T. Saito, A. Takasaki, Trans. Mater. Res. Soc., Jpn. 34 (3) (2009) 403–406.
[11] J. Rodriguez-Carvajal, Physica B 192 (1993) 55–69.
[12] J.L. Soubeyroux, D. Fruchart, G. Lorthioir, P. Ochin, D. Colin, J. Alloys Compd. 196 (1993) 127–132.
[13] D. Noreus, P.E. Werner, K. Alasafi, E. Schmidt-Ihn, Int. J. Hydrogen Energy 10 (1985) 547–550.
[14] K. Kudoh, M. Tokonami, S. Miyazaki, K. Otsuka, Acta Metall. 33 (11) (1985) 2049–2056.